ORIGINAL ARTICLE

Long-Term Adaptation to Galactose as a Sole Carbon Source Selects for Mutations Outside the Canonical *GAL* Pathway

Artemiza A. Martínez[1] · Andrew Conboy[1] · Sean W. Buskirk[2] · Daniel A. Marad[1] · Gregory I. Lang[1]

© The Author(s), under exclusive licence to Springer Science+Business Media, LLC, part of Springer Nature 2022

Abstract

Galactose is a secondary fermentable sugar that requires specific regulatory and structural genes for its assimilation, which are under catabolite repression by glucose. When glucose is absent, the catabolic repression is attenuated, and the structural *GAL* genes are fully activated. In *Saccharomyces cerevisiae*, the *GAL* pathway is under selection in environments where galactose is present. However, it is unclear the adaptive strategies in response to long-term propagation in galactose as a sole carbon source in laboratory evolution experiments. Here, we performed a 4,000-generation evolution experiment using 48 diploid *Saccharomyces cerevisiae* populations to study adaptation in galactose. We show that fitness gains were greater in the galactose-evolved population than in identically evolved populations with glucose as a sole carbon source. Whole-genome sequencing of 96 evolved clones revealed recurrent de novo single nucleotide mutations in candidate targets of selection, copy number variations, and ploidy changes. We find that most mutations that improve fitness in galactose lie outside of the canonical *GAL* pathway. Reconstruction of specific evolved alleles in candidate target of selection, *SEC23* and *IRA1*, showed a significant increase in fitness in galactose compared to glucose. In addition, most of our evolved populations (28/46; 61%) fixed aneuploidies on Chromosome VIII, suggesting a parallel adaptive amplification. Finally, we show greater loss of extrachromosomal elements in our glucose-evolved lineages compared with previous glucose evolution. Broadly, these data further our understanding of the evolutionary pressures that drive adaptation to less-preferred carbon sources.

Introduction

Catabolic repression–the inability to utilize a less-preferred carbon source when a more favorable one is present–is a core principle of metabolic gene regulation. The standard example is the *lac* operon in *E. coli* where expression of the structural genes needed to assimilate alternative carbon sources require that two conditions be met: the absence of the preferred carbon source and the presence of the alternative carbon source (Jacob and Monod 1961). This logic is used to regulate the assimilation of a variety of secondary

fermentable (e.g., sucrose, maltose, and galactose) and non-fermentable (e.g., acetate, glycerol, and ethanol) carbon sources (Zaman et al. 2008; Fendt and Sauer 2010).

In the yeast, *Saccharomyces cerevisiae*, galactose is a widely used secondary carbon source. Galactose is a common sugar found in dairy products, fruits, grains, and vegetables (Acosta and Gross 1995; Lee et al. 2011). Galactose assimilation requires three regulatory genes and four structural genes, which are expressed only when glucose is absent and galactose is present. In the absence of glucose, the Snf1 complex attenuates catabolite repression by phosphorylating the Mig1 transcriptional repressor, leading to its inactivation (Conrad et al. 2014; Nair and Sarma 2021). Full activation of galactose structural genes is mediated by a transcription factor (Gal4p), a repressor (Gal80p), and a co-inducer (Gal3p). In the absence of galactose, Gal80p sequesters Gal4p in the cytoplasm. When present, galactose binds to Gal3p, which in turn binds to Gal80p, releasing Gal4p. Once released, Gal4p relocalizes to the nucleus and increases up to ~1000-fold the transcription of the *GAL* structural genes, which

Handling editor: **Kerry Geiler-Samerotte**.

✉ Gregory I. Lang
glang@lehigh.edu

1 Department of Biological Sciences, Lehigh University, Bethlehem, PA, USA

2 Department of Biology, West Chester University, West Chester, PA, USA

are clustered in a 7 kb region on Chromosome II (Sellick et al. 2008).

Galactose initially enters the cell through low-affinity hexose transporters (Escalante-Chong et al. 2015). However, once the switch occurs, galactose enters the cell predominantly through the high-affinity galactose transporter Gal2 (Conrad et al. 2014). Once in the cell, three main enzymes are necessary to catalyze four sequential steps in galactose assimilation. Gal1p is the galactokinase. Gal10p contains two catalytic domains: a mutarotase that interconverts galactose enantiomers and an epimerase that converts UDP-galactose to UDP-glucose. Gal7p is the galactose-1-phosphate uridylyltransferase. These enzymes are tightly regulated to reduce their costly expression and avoid accumulation of the toxic intermediate galactose-1-phosphate (Slepak et al. 2005; Wang et al. 2015).

The genetic switch from glucose to galactose utilization has been extensively studied as a model system to understand the evolution of gene clustering (Hittinger and Carroll 2007, Lang and Botstein 2011, Harrison et al. 2021), transcriptional regulation (van denBrink et al. 2009; New et al. 2014; Peng et al. 2015), nutrient-sensing metabolism (Escalante-Chong et al. 2015; Lee et al. 2017), and cellular memory (Acar et al. 2005; Sood and Brickner 2017). The clustering and regulation of the *GAL* pathway has evolved independently multiple times in fungi. Relative to other yeast, *S. cerevisiae* evolved strong repression and slow induction of the *GAL* genes, which confers a fitness advantage in environments where glucose is in excess (Harrison et al. 2021). However, studies on natural environments identified novel strategies in *S. cerevisiae* isolates that are associated with improved growth on galactose. For example, natural variation in catabolite repression varies with the length of diauxic lag such that galactose is only assimilated once glucose drops below a certain threshold (Wang et al. 2015). Lineages isolated from dairy products harbor *GAL* variation, such as *GAL3* polymorphisms, *GAL2* amplification, and *GAL* cluster introgressions from *S. paradoxus* reflecting adaptation to a galactose-rich environment (Duan et al. 2018; Legras et al. 2018; Boocock et al. 2021). These suggest that the structural and regulatory genes in the *GAL* pathway are under selection in environments where galactose is present. However, natural environments are complex and variable environments; therefore, it is unclear how selection acts to improve the growth in a simple environment containing galactose as the sole carbon source.

Experimental evolution of microbes is a powerful tool to identify genomic changes during adaptation in different environments (Voordeckers et al. 2015; Swamy and Zhou 2019). The molecular targets of selection can be informative on the pressure that drive adaptation in each system. For example, in glucose-limitation laboratory evolution, recurrent mutations arise in nutrient signaling pathways, such

as the Ras/PKA pathway and TOR pathway (Venkataram et al. 2016). In chemostat, amplification of glucose transporters is another recurrent adaptive mechanism (Kao and Sherlock 2008; Wenger et al. 2011). In glucose-rich laboratory evolution, genetic targets of selection are involved in cell wall biogenesis, assembly, and cytokinesis, as well as nutrient sensing and signaling (Lang et al. 2013; Fisher et al. 2018; Marad et al. 2018; Johnson et al. 2021). Previous laboratory evolution experiments in galactose have identified mutations in genes encoding the transcriptional repressor *GAL80* (Quarterman et al. 2016), proteins involved in polarized growth (Jerison et al. 2020), and regulators of the Ras/PKA pathway (Hong et al. 2011; Hong and Nielsen 2013). In contrast to variation found in galactose-rich natural environments, mutations identified in laboratory evolution are predominantly outside the canonical *GAL* genes.

Previously, we evolved 48 diploid populations in glucose over 4,000 generations (Marad et al. 2018). Here, we perform an identical 4,000-generation diploid evolution experiment using galactose as the sole carbon source. We directly compare the rates of adaptation and genetic targets of selection between glucose and galactose evolution. Consistent with previous work, we find that most mutations that improve fitness in galactose lie outside of the canonical *GAL* pathway. In addition, we identify recurrent copy number variants, including aneuploidies on Chromosome VIII. Reconstruction of specific evolved alleles in *SEC23* and *IRA1* showed significant increases in fitness under galactose conditions. Finally, we show multiple losses of extrachromosomal elements, two of which (2-micron plasmid and Killer phenotypes) were also observed in galactose-evolved populations, and one of which (mitochondrial genome) was not.

Results

Higher Rate of Adaptation in Rich Galactose Medium Compared to Rich Glucose Medium

To determine the evolutionary response to constant growth in an alternative carbon source, we evolved 48 replicate populations of the same diploid ancestor in a rich medium with galactose as the sole carbon source (YPGal). After 2,000 generations, all populations increased in fitness compared to the ancestor (Fig. 1A) with a mean fitness gain of $8.2 \pm 0.1\%$ ($\alpha = 0.05$). This is significantly greater than the fitness gains for the identically evolved populations using glucose as a sole carbon source ($p < 0.0001$, Wilcoxon rank-sum test; Fig. 1B), which showed mean fitness gains of $3.7 \pm 0.06\%$ ($\alpha = 0.05$) in the first 2,000 generations of evolution.

To identify mutations that arose in the galactose-evolved populations, we sequenced two clones from each of the 48 populations at Generation 4,000. We found 2,406 de novo
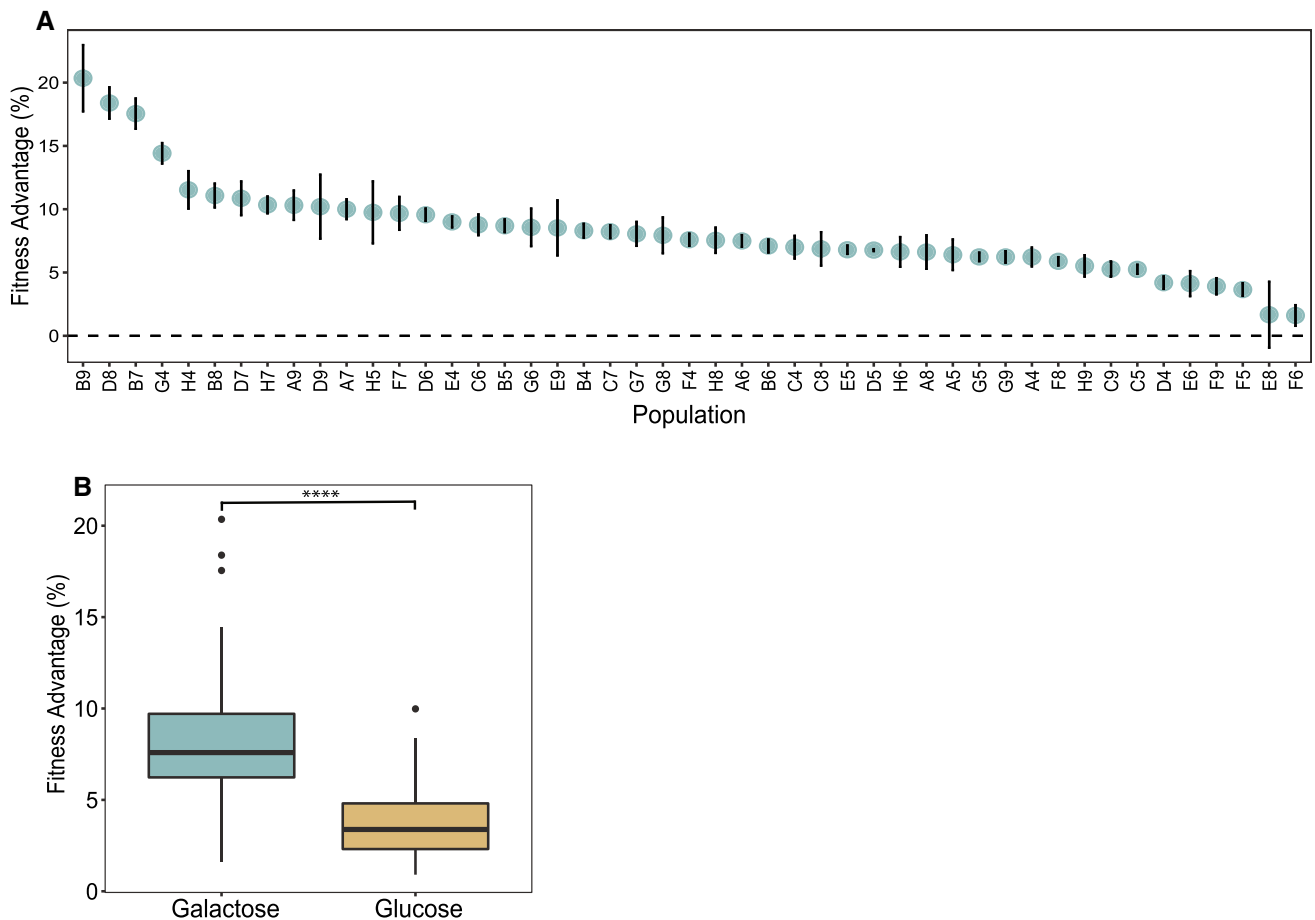
Fig. 1 Galactose-evolved populations have a higher fitness advantage after 2,000 generations of laboratory evolution. **A** Relative fitness advantage of 48 evolved populations on galactose. Vertical error bars reflect ± standard error of the regression. **B** Adaptation in galactose has a significantly higher fitness advantage compared with glucose-evolved populations ($p < 0.0001$, Wilcoxon rank-sum test). Box plot reflects the mean fitness of 48 populations in both conditions. Galactose populations have a mean fitness advantage of 8.2%, whereas glucose populations have a mean of 3.7%. Glucose fitness data are from Marad et al. 2018

mutations across 96 evolved clones distributed across all 16 chromosomes with a mean of 25 ± 6 mutations per clone. Of these mutations, 794 are present in both clones from the same population, and 735 mutations are only found in one clone.
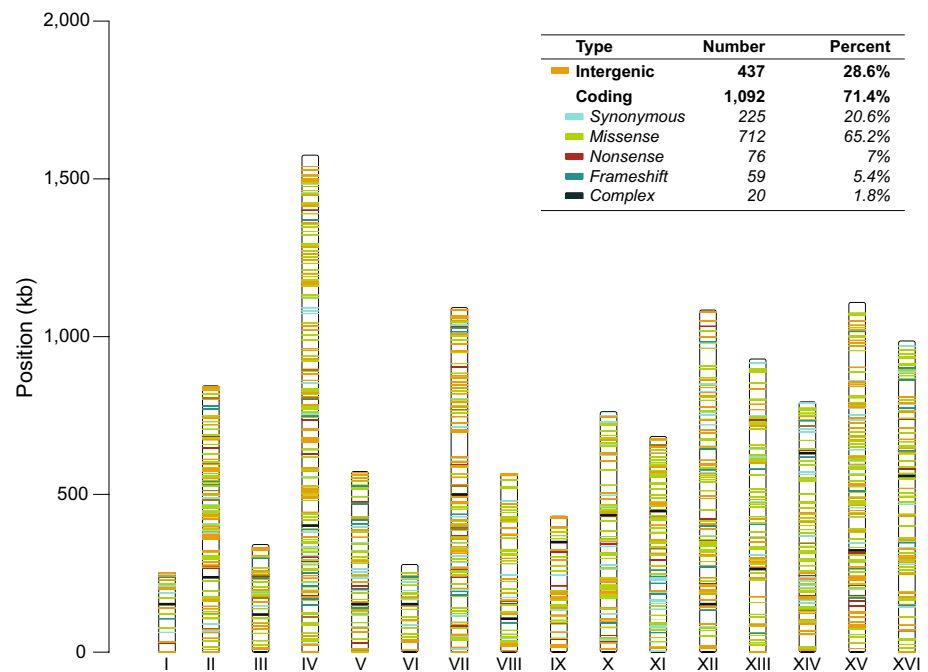
Of the 1,529 unique mutations, 91% are single nucleotide polymorphisms, most of which are in coding genes (1092 out of 1529; 71.4%). 712 of these mutations are mostly missense (46.6%), 225 are synonymous (14.7%), 76 are nonsense (5%), 59 are frameshift (3.9%), and 20 are complex mutations (1.3%) (Fig. 2 and Supplementary Data). Consistent with our previous work (Fisher et al. 2018; Marad et al. 2018), we find that heterozygous mutations outnumber homozygous mutations ~ 19:1 (Supplementary Fig. 1A), and that homozygous mutations are clustered on the right arm of Chromosome XII (Supplementary Fig. 1B). This region is a hotspot for loss of heterozygosity (LOH) due to the rDNA

locus: approximately one third of the homozygous mutations are located on this chromosome.

Beneficial Mutations are Commonly Found Outside the Canonical GAL Pathway

To identify the pathways under selection in galactose medium we performed Gene Ontology (GO) enrichment using all 860 coding genes that were mutated across all populations. This analysis showed, at a broad level, an enrichment for genes involved in: positive regulation of the metabolic process, cellular response to stimulus, intracellular signal transduction, and cellular component organization (biological process enrichment, $p < 0.001$). We next restricted our GO-term enrichment analysis to the 24 genes that acquired mutations in three or more populations. This showed enrichment for genes involved in the negative regulation of Ras signal transduction including *IRA1*, *IRA2*, and

Fig. 2 The spectrum of mutations in 96 evolved clones under galactose evolution. Distribution of 1,529 unique evolved mutations across 16 Chromosomes. The vertical bars represent each Chromosome labeled by Roman numeral. The horizontal lines reflect each mutation colored based upon their protein-coding effect (top box). Other mutations group conservative inframes, disruptive inframes, and complex mutations. Centromers are represented with a black horizontal line

Type	Number	Percent
Intergenic	**437**	**28.6%**
Coding	**1,092**	**71.4%**
Synonymous	*225*	*20.6%*
Missense	*712*	*65.2%*
Nonsense	*76*	*7%*
Frameshift	*59*	*5.4%*
Complex	*20*	*1.8%*

BEM2 ($p < 0.005$). In addition, we found mutations in *GPB1*, *PDE2*, and *CDC25* in one or two populations. All the mutations found in Ras pathway genes are nonsynonymous.

We identified individual genes that are targets of selection by determining which genes are mutated more often than expected by chance across replicate populations. Using this approach, we identified five targets of selection with a $p < 0.001$ (Fig. 3A). These five genes are involved in the Ras/PKA pathway (*IRA1*), histone deacetylation (*SNT1*), endosome organization/vacuolar biogenesis (*PEP5*), secretory pathway (*SEC23*), and actin filament (*BNI1*). Notably, we did not find a GO enrichment or a significant number of mutations in genes with an obvious connection to galactose metabolism. We found two missense and one conservative inframe in *GAL10*, two missense mutations in *GAL2*, one missense mutation in *GAL4*, one missense mutation in *GAL7*, one nonsense and one synonymous in *GAL1*. None of these genes, however, were acquired more mutations than expected by chance at $p < 0.001$. None of the candidate targets of selection in galactose are significantly overrepresented in glucose evolution experiment and vice versa (Fig. 3B). The most common targets of selection in glucose-evolved populations are cell wall-associated genes, *CTS1*, *ACE2*, and *RPL33A* ($p < 0.001$, Poisson distribution; Fig. 3B). Of these, only one mutation in *ACE2* was observed in one galactose-evolved population.

Based on the types of mutations observed, we can determine how selection is acting on the candidate targets of selection (Table 1). We observed enrichment for nonsense and frameshift mutations (high impact mutations) in *SEC23*, *PEP5*, and *IRA1*, suggesting selection for loss-of-function.

In contrast, we only observe missense mutations in *SNT1*. Out of the five mutations found in *BNI1,* three are synonymous and conservative inframe mutations, suggesting that this locus may not have a strong effect in the adaptation of galactose. Though there are a few notable exceptions of beneficial synonymous mutations in other systems (Bailey et al. 2014; Kristofich et al. 2018), most synonymous mutations in our system are neutral (Buskirk et al. 2017) and reach high frequency by genetic hitchhiking (Lang et al. 2013). Ignoring synonymous mutations removes a large background of hitchhiker mutations and produces more robust predictions of true targets of selection. If we restrict our analysis to nonsynonymous mutations, *PEP5* and *BNI1* are no longer significant at $p < 0.001$ (Supplementary Data).

Galactose-Evolved Alleles Show Carbon Source Dependence Effect

To quantify the fitness effect of individual mutations, we reconstructed evolved mutations in putative targets of selection (*snt1*-A168S, *snt1*-R1009K, *sec23*-R592I, *ira1*-S700P, Table 1) as well as evolved mutations in the galactose pathway (*gal10*-D302N, *gal10*-R433P, *gal7*-Q265E, and *gal1*-G347*, Supplementary Fig. 3B) even though our statistical analysis did not identify them as candidate targets of selection. Each mutation was reconstructed in the ancestral background as haploids, heterozygous diploids, and homozygous diploids. As a control, we constructed two previously identified adaptive mutations, *hsl1*-A262P (Buskirk et al. 2017; Vignogna et al. 2021), and *ace2*-R669* (Marad et al. 2018)
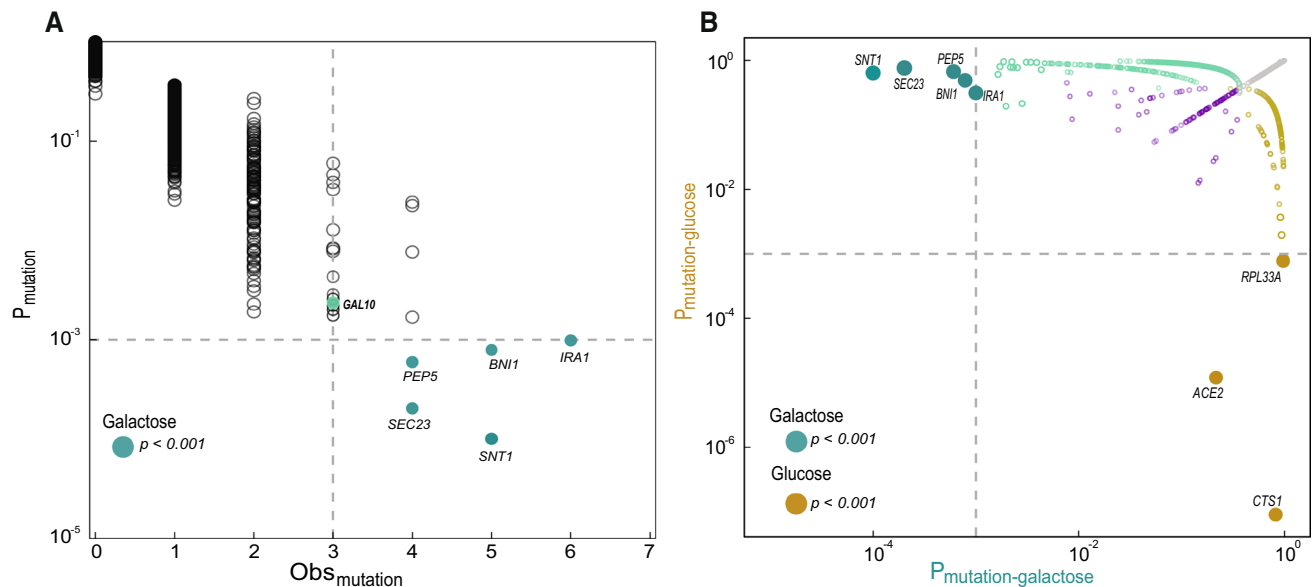
Fig. 3 Common targets of selection in galactose-evolved populations. **A** Plotted on the x-axis is the observed number of coding sequence (CDS) mutations in each of the 5800 genes. The y-axis is the probability that the observed number of CDS mutations in each gene (without mutation type distinction) occurred by chance. We used a Poisson distribution weighted for the length of each gene (Fisher et al. 2018). The gray dotted line indicates the cut-off of genes with 3 or more CDS mutations with corresponding *p*-value < 0.001 (solid dark cyan). Genes in this area are common targets of selection. We also denoted gal10 with *p*-value = 0.002 (solid light green). **B** Com-

mon targets of selection in galactose-evolved populations differ from glucose-evolved populations. Plotted is the ratio of the probability that the observed number of CDS mutations in a gene occurred by chance in galactose populations (cyan circles) versus glucose populations (gold circles). The gray dotted line indicates the cut-off genes with a *p*-value < 0.001. Targets of selection were labeled with the gene name and bigger solid dark cyan circles. Open purple circles indicate CDS mutated in both conditions. Gray circles indicate CDS that were not mutated under any conditions. Glucose data are from Marad et al. 2018

Table 1 Common targets of selection in galactose-evolved populations

Gene	*p*-value[a]	Amino acid change	Zygosity	Clone[b]	Biological process (SGD)
SNT1 (Chr III)	4.55–04	Ala168Ser[d]	Heterozygous	**F51, F52**	Subunit of the Set3C deacetylase complex
		Val237Ile	Heterozygous	B42	
		Val374Leu	Heterozygous	**E81, E82**	
		Arg1009Lys[d]	Heterozygous	**A91, A92**	
SEC23 (Chr XVI)	8.01–05	Gln167[c]	Heterozygous	**F41, F42**	COPII vesicle coating
		Gln494[c]	Heterozygous	**A91, A92**	
		Arg592Ile[d]	Heterozygous	**G61, G62**	
		Leu701fs	Heterozygous	**H61, H62**	
IRA1 (Chr II)	2.84–04	Ser700Pro[d]	Homozygous	**C41, C42**	Inhibitory
		Gln933[c]	Homozygous	**H81, H82**	Regulator of the RAS-cAMP pathway
		Pro1013fs Leu1402[c]	Heterozygous	**A91, A92**	
		Gln2083[c]	Heterozygous	**G91, G92**	
		Ala2292Ser	Heterozygous	**A61, A62**	
			Heterozygous	**B51, B52**	

Bolded clones indicate the SNP was found in all clones of the population

[a]Statistical analysis focus on nonsynonymous mutations

[b]Clones indicate the well ID followed by the clone number

[c]Nonsense

[d]Reconstructed mutations

fs Frameshift

from haploid-glucose evolution and diploid-glucose evolution, respectively.

We performed competitive fitness assays of the reconstructed strains against a fluorescently labeled ancestral

reference in both galactose and glucose. Reconstruction of heterozygous evolved mutations in the *GAL* pathway does not show fitness advantage in galactose (Supplementary Fig. 3B). We observed the same pattern for the homozygous reconstruction. In contrast, for all evolved mutations identified in our candidate targets of selection, we find that the fitness effects in glucose and galactose are highly correlated ($r = 0.69$, $p = 0.0122$, Pearson correlation coefficient; Supplementary Fig. 2). Nevertheless, the magnitude of the fitness effect was greater in the condition in which the specific mutation arose, and this difference is more exaggerated for homozygous mutations. We found a fitness advantage of the heterozygous *sec23*-R592I mutation of $3.9 \pm 0.4\%$ ($\alpha = 0.05$; $p < 10^{-6}$ one-way ANOVA, Tukey's HSD test) in galactose than glucose and a larger fitness advantage of $6.2 \pm 0.5\%$ ($\alpha = 0.05$; $p < 10^{-8}$, one-way ANOVA, Tukey's HSD test) as homozygous in galactose compared to glucose. We observed similar fitness advantage for *ira1*-S700P mutation; $3.3 \pm 0.3\%$ ($\alpha = 0.05$; $p < 10^{-3}$, one-way ANOVA, Tukey's HSD test) as heterozygous and $5.3 \pm 0.3\%$ ($\alpha = 0.05$; $p < 10^{-8}$, one-way ANOVA, Tukey's HSD test) as homozygous (Fig. 4B). Despite the greater fitness benefit of the homozygote mutations, only *ira1*-S700P lost heterozygosity in the evolution experiment. Surprisingly, neither of the two *SNT1* alleles provided a selective benefit in galactose or glucose. The heterozygous *snt1*-R1009K mutation is strongly deleterious, but it is neutral as a homozygote. The *snt1*-A592S shows the opposite pattern: the heterozygous mutation is neutral but homozygous mutation is deleterious (Fig. 4). As expected, the ploidy, glucose-evolved alleles of *hsl1*-A262P and *ace2*-R669* are more beneficial in glucose although both alleles also improved fitness in galactose (Fig. 4 and Supplementary Fig. 3). Our results show that

evolved mutations on *SEC23* and *IRA1* are beneficial only in the condition in which they arose.

## Aneuploidies and CNVs are Common in Galactose-Evolved Populations

In addition to point mutations, copy number variants (CNVs) and aneuploidies can contribute to adaptation (Gresham et al. 2008; Yona et al. 2012; Sunshine et al. 2015). To identify CNVs and aneuploidies in our galactose-evolved populations, we calculated the relative coverage across all 16 chromosomes. We find that most of our evolved clones (28/46; 61%) have one or two extra copies of Chromosome VIII. In addition, we find one population with monosomy for Chromosome I (Fig. 5). We validated these findings by sequencing eight random clones by long-read sequencing (Supplementary Fig. 4A). Although the high occurrence of additional copies for Chromosome VIII strongly suggests an adaptive strategy under galactose, populations with extra copies do not correlate with higher fitness than euploid populations ($p = 0.56$, Wilcoxon rank-sum test; Supplementary Fig. 4B).

In addition to loss or gain of entire chromosomes, we also detect large (> 40 kb) CNVs in our evolved clones, including eight unique amplifications and two deletions (Table 2 and Supplementary Fig. 5). We identified several populations with CNVs in the right arm of Chromosome II; however, in only population does the amplification include the *GAL1-GAL10-GAL7* gene cluster (Population A4, Chromosome II: 268,984–275,164). No other recurrent CNVs were identified that overlap with *GAL* genes (Table 2 and Supplementary Fig. 5). In Populations A4 and B9, we identified duplication of genes associated with Ras/PKA signaling pathway; *IRA1* (Chromosome II: 534,751–544,029) and
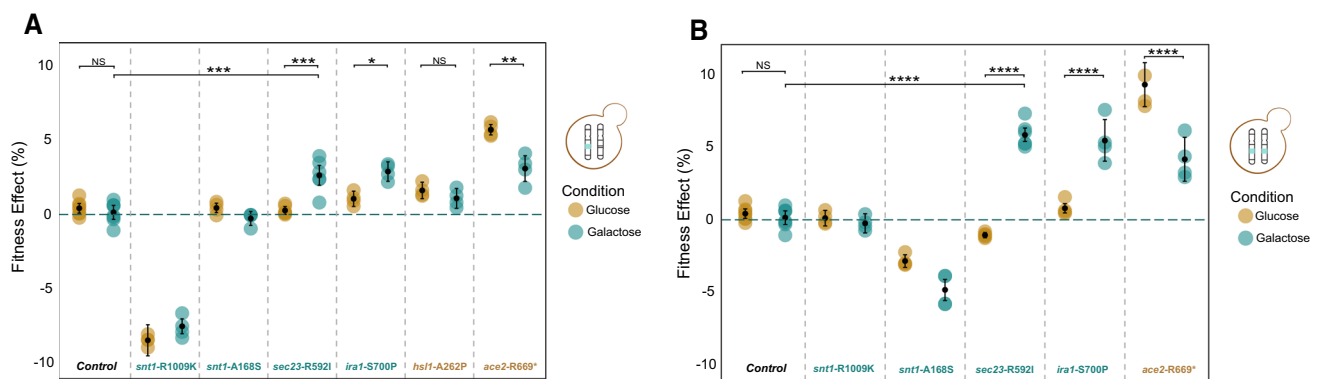
Fig. 4 Galactose-evolved mutations show variation in fitness effect and carbon source dependence. Average fitness effects of the reconstructed mutations in snt1 ($n = 4$), sec23 ($n = 6$), and ira1 ($n = 4$) in both zygosities; **A** heterozygous and **B** homozygous mutations. Fitness effect were compared with wild-type version ($n = 6$), hsl1 mutation ($n = 4$) from glucose, haploid evolution (Fisher et al. 2018), and

ace2 mutation ($n = 4$) from glucose, diploid-evolution (Marad et al. 2018). We were not able to generate hsl1 homozygous mutation. The sec23-R592I has a significant fitness gain in galactose compare to glucose. Asterisk (****) indicate $p < 10^{-8}$, (***) $p < 10^{-5}$, (**) $p < 10^{-4}$, (*) $p < 10^{-3}$, and NS: not significant; one-way ANOVA, tukey's HSD test. Error bars are the s.e.m
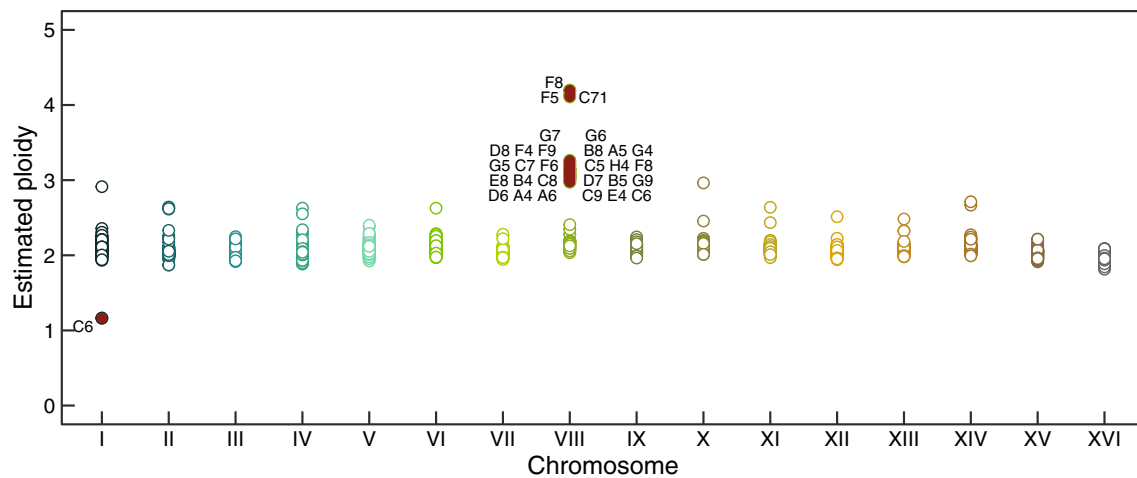
Fig. 5 Aneuploidy on Chromosome VIII appears to be a parallel evolutionary adaptation in the galactose condition. To estimate the ploidy of 96 clones, we calculated the median coverage across each chromosome compared to genome-wide coverage. Baseline ploidy is 2 N. Aneuploidies are shown as filled red circles and labeled by name population. Empty circles indicate euploid. Notably, duplication of Chromosome VIII occurred in 28 populations out of 46 populations

Table 2 Structural variants in galactose-evolved populations

Chr	Start (kb)	Stop (kb)	Length (kb)	Copy number	Class	Clone[b]
I	0	161,000	161	1 N	Aneuploidy	**C61, C71**[c]
II[1,3]	226,000	844,051	618	3 N	CNV	**A41, A42**[c]
II	666,000	836,000	170	3 N	CNV	**B61, B62**
II[3]	354,000	836,000	482	3 N	CNV	**H71, H72**
II	737,000	844,051	107	1 N	CNV	**G71, G72**
VII	749,000	1,092,105	343	3 N	CNV	**D51, D52**
VIII[2]	0	844,051	844	3 N & 4 N	Aneuploidy	**G71, G72, G61, G62, D81, D82, F41, F42, F91, F92, B81, B82, A51, A52, G41, G42, G51, G52, C71**[c]**, C61**[c]**, F61**[c]**, F62**[c]**, F71**[c]**, C51, C52, H41, H42, F81, F82, E81, E82, B41, B42, C81, C82, D71, D72, B51, B52, G91, G92, D61, D62, A41**[c]**, A42**[c]**, E71**[c]**, E72**[c]**, A61, A62, C91, C92, E41, E42, C61**[c]**, C721**[c]**, D91, D92**
X[2]	502,000	762,303	260	4 N	CNV	**G41,G42**
XI	0	297,000	297	3 N & 4 N	CNV	**H91, H92**, H82
XIII	379,000	750,000	371	3 N	CNV	F52
XIII	0	44,000	44	3 N	CNV	**D41, D42**
XIV[2,3]	0	479,001	479	3 N	CNV	**B91, B92**

Bolded population indicates that the CNV was found in all clones of the population

[b]Clones indicate the well ID followed by the clone number

[c]Populations with cross-contamination (See Supplementary Data)

[1]Duplication of the GAL cluster. Coordinates: chrII. 268,984–275,164, W303 ref

[2]Duplication of hexose transporters

[3]Duplication of components of the Ras/PKA pathway

RAS2 (Chromosome XIV: 440,898–441,866), respectively. Additionally, we found amplifications of regions containing hexose transporters genes; *HXT14* (Population B9), *HXT9, HTX8, HXT16* (Population G4), *HXT4, HXT1*, and *HXT5* (populations with aneuploidies for Chromosome VIII).

These data demonstrate recurrent amplifications of regions that contain genes encoding hexose transporters, suggesting a potential adaptive mechanism in our galactose evolution. We do not, however, find a significant correlation between

higher fitness and CNVs ($p = 0.89$, Wilcoxon rank-sum test; Supplementary Fig. 4B).

Changes in Copy Number of Extrachromosomal Elements and Reduction of the Killer Phenotype in Galactose-Evolved Populations

In addition to evolution in the nuclear genome, we determined the extent to which cytoplasmic elements (the mitochondrial genome, the 2-micron plasmid, and the yeast dsRNA Killer virus) changed during evolution in galactose. Using read depth as a proxy, we estimated the copy number of mitochondrial DNA for each clone according to Chiara et al. 2020. Estimates of mitochondrial copy number is highly correlated between clones from the same population ($r = 0.928$, $p < 0.0001$, Pearson correlation; Supplementary Fig. 7A). Most of the populations show a significant decrease in the mitochondrial copy number ($p < 0.0001$, Wilcoxon rank-sum test), with a global mean of ~ 8:1 mitochondrial to nuclear genomes (Supplementary Fig. 6A) and with only six galactose-evolved populations maintaining or increasing mitochondrial copy number (19:1 ratio between mitochondrial and nuclear genomes). In contrast mitochondrial copy number is maintained throughout evolution in glucose-evolved populations (Supplementary Fig. 7C).

Like mitochondrial copy number, our estimates of the 2-micron plasmid copy number are highly correlated between clones from the same population ($r = 0.66$, $p < 0.0001$, Pearson correlation; Supplementary Fig. 7B). Our galactose-evolved populations show a drastic loss of 2-micron copy number (from 133 initial copies to an average of 57 copies per every copy of the nuclear genome). Only three populations showed a higher 2-micron copy number than the ancestor (Supplementary Fig. 6B). We did not observe differences in reduction of 2-micron copy number between galactose and glucose-evolved populations ($p = 0.43$, Wilcoxon rank-sum test; Supplementary Fig. 7D). We also did not find correlation between reduction of mitochondrial DNA and 2-micron ($r = -0.07$, $p = 0.48$, Pearson correlation).

As a proxy for the loss of the killer toxin, we quantified killing ability in our populations (Buskirk et al. 2020). Similar with glucose evolution, we find that the majority of the populations (42/48) lost totally or partially the killer-associated phenotype (Supplementary Fig. 6C, Supplementary Fig. 8). We did not observe a significant difference of the loss of the killer phenotype between both conditions ($p = 0.17$, Wilcoxon rank-sum test). Consistent with previous glucose evolution, reduction of the 2-micron and killing ability is also a common mechanism in our galactose evolution adaptation. In contract, mitochondrial DNA has recurrent losses only in galactose evolution.

Discussion

The genetic switch from glucose to galactose utilization in *S. cerevisiae* has been extensively studied (Acar et al. 2005, Ronen and Botstein 2006, van den Brink et al. 2009, Escalante-Chong et al. 2015). However, the strategies for long-term adaptation to galactose as a sole carbon source are not well understood. To determine how galactose affects adaptation in budding yeast, we evolved 48 diploid populations in rich galactose medium under identical conditions to our previous glucose evolution experiment (Marad et al. 2018). We show that fitness gains over the first 2,000 generations were greater in the galactose medium compared to glucose. We find that beneficial mutations in the galactose-evolved populations are beneficial in glucose medium but that the magnitude of the benefit is smaller. Similarly, glucose-evolved mutations are strongly beneficial in glucose, but beneficial in galactose, suggesting that environment-specific selective pressures drive the fixation of specific mutations in each environment. These results are consistent with findings of others showing a positive correlation between fitness in glucose and fitness in galactose (Chen and Zhang 2020; Jerison et al. 2020).

To identify the targets of selection during long-term growth on galactose, we sequenced two clones from each population after 4,000 generations. Several studies have identified functional variants in the *GAL* pathway that tune the response of the galactose pathway in natural populations (Roop et al. 2016; Lee et al. 2017; Boocock et al. 2021). It is, therefore, reasonable to expect laboratory adaptation to constitutive galactose to select for mutations in these same genes. While we did observe several mutations in the *GAL* pathway genes, we do not observe more mutations than expected by chance, and reconstruction experiments failed to identify a fitness advantage (Supplementary Fig. 3B).

We identify candidate targets of selection outside of the canonical galactose pathways, with *SNT1, SEC23,* and *IRA1* as the most significant hits. *IRA1* is repeatedly observed as a target of selection across evolution experiments (Lang et al. 2013; Fisher et al. 2018; Li et al. 2018; Johnson et al. 2021), whereas *SNT1* is rarely observed (Fisher et al. 2018). *SEC23* has not been previously identified as recurrent mutated gene in glucose. These three genes show enrichment of missense and nonsense mutations consistent with being under selection in galactose. In diploid evolution experiments, beneficial mutations are partially dominant or overdominant (Aggeli et al. 2022). Reconstruction of evolved alleles shows that *ira1*-S700P and *sec23*-R592I are partially dominant. Consistent with being partially dominant, we find that the allele *ira1*-S700P fixed as a homozygote. It is not surprising that *sec23*-R592I did not undergo loss of heterozygosity

since the majority of mutations in the evolved clones are heterozygous (1,444 of 1,529 mutations).

IRA1 is a negative regulator of the Ras/PKA signaling pathway, one of the best-known glucose-triggered signaling cascades (Tamanoi 2011; Broach 2012). The Ras pathway is a hotspot for functional variation owing to its role in regulating metabolic, transcriptional, and physiological responses to nutrient availability. Because of this, genes in the Ras pathway are common targets of selection in nearly all yeast evolution experiments including rich glucose medium (Lang et al. 2013), defined low glucose medium (Venkataram et al. 2016), as well as glucose-limited (Kvitek and Sherlock 2013) and nitrogen-limited (Hong and Gresham 2014) chemostats.

Mutations identified in experimental evolution are often pleiotropic, affecting fitness (either positively or negatively) in other environments (Ostrowski et al. 2005; Jerison et al. 2020; Bakerlee et al. 2021). Mutations in the Ras pathway have been shown to result in fitness tradeoffs under alternative carbon sources (Hong et al. 2011; Hong and Nielsen 2013) or prolonged starvation (Li et al. 2018). Here, we find that the galactose-evolved mutation, *ira1*-S700P, has a greater fitness benefit in galactose compared in glucose. These results suggest that though the Ras/PKA pathway is a general hub for adaptive mutations in all laboratory evolution experiments, individual mutations are condition specific, adjusting cell physiology match the environment.

Outside of the Ras/PKA pathway, the secretory pathway is another common target of selection in galactose. Apart from recurrent mutations in *SEC23*, we observe independent moderate-impact mutations in six more genes that encode secretory proteins. The endoplasmic reticulum has a role in maintaining metabolic homeostasis by sensing nutrient availability (Fu et al. 2012). Another common target of selection is *SNT1*, which encodes a histone deacetylase. However, despite *SNT1* being a common target of selection, neither of our reconstructed *SNT1* mutations are beneficial on their own (Fig. 4). It is possible the presence of epistasis interactions between *SNT1* mutations and the genetic background. The *snt1*-A1009S and *snt1*-V237I mutations arose in populations with mutations in *ira1* and *ira2*, respectively. Genetic interaction among co-evolved mutations is common in experimental evolution (Fisher et al. 2019; Vignogna et al. 2021).

Increasing the copy number of specific genes whose expression level is limiting is another common mode of adaptive evolution. For example, the amplification of transporter and specific permeases are a recurrent adaptive mechanism to selection in medium limited for glucose (Gresham et al. 2008; Kao and Sherlock 2008), nitrogen (Hong and Gresham 2014), sulfur (Sunshine et al. 2015), or raffinose (Scott et al. 2017). An essential step in utilizing galactose is its transport achieved by Gal2p, a closely related hexose transporter (Boles and Hollenberg 1997). Notably, we did not detect any duplications of the transporter *GAL2* located on Chromosome XII. Of the four CNVs on Chromosome II, only the largest one encompasses the *GAL1-GAL10-GAL7* gene cluster (Supplementary Fig. 5). We do, however, find that 61% of our populations have fixed aneuploidies on Chromosome VIII. We suggest that a strong adaptive advantage in our populations can be explained by the amplification of hexose transporters on Chromosome VIII: *HXT4, HXT1, and HXT5*. Under galactose conditions, selection for spontaneous duplication of Chromosome VIII may favor nutrient transporters, leading to more efficient nutrient uptake into central metabolism (Torres et al. 2007). We only detected one point mutation in any of the *HXT* genes (a single missense mutation in *HXT3*).

Most of the observed adaptive processes have focused on the nuclear genome. Little is known about the evolution of extrachromosomal elements in different environments. Changes in copy number can give us a first light of whether these elements are under selection or not. Recently, Johnson et al. 2021 showed the recurrent loss of 2-micron plasmids and reduction of the killer phenotype of the Killer virus under rich glucose and synthetic complete media. Here we find a similar pattern in 2-micron plasmids and Killer-associated phenotypes in galactose-evolved populations (Supplementary Fig. 6). The selective benefit decreasing 2-micron copy number are unclear; however, we previously showed that the loss of Killer virus occurs due to an intracellular fitness advantage of viruses that do not produce toxin (Buskirk et al. 2020).

We observe multiple losses of mitochondrial DNA (Supplementary Fig. 6). When growing on galactose, *S. cerevisiae* does not exhibit a Kluyver effect (inability to grow on and ferment sugars under anaerobic conditions). Therefore, it can consume galactose under respiration and fermentation (van den Brink et al. 2009). The existence of this respiration-dependent assimilation of sugars is an essential link between mitochondria and sugar utilization (Quarterman et al. 2016). The reduction of mitochondrial genome copy number may indicate that the evolved populations are increasing fermentation relative to respiration. Mitochondrial genome copy number, however, is dynamic with considerable strain-to-strain variation (Galeota-Sprung et al. 2022). We, therefore, cannot determine if the changes we observe are adaptive or are a secondary response to changes in growth.

Overall, we find that long-term adaptation to growth on galactose is driven mainly by mutations outside of the canonical *GAL* pathway. Specifically, we identify Ras/PKA signaling as a major target of selection, as it is in nearly all environments. We find that glucose and galactose-evolved alleles are more beneficial in the condition in which they arose. Unlike in glucose-evolved populations, we find recurrent aneuploidy for Chromosome VIII suggestion a potential

role in galactose adaptation by increasing the copy number of *HXT* genes. We observe a reduction in 2-micron copy number, mitochondrial copy number, and killing ability across our evolved populations.

Methods

Strains Construction

All strains used in this study are derived from the W303 background (*ade2-1, CAN1, his3-11, leu2-3,112, trp1-1, URA3, bar1Δ::ADE2, hmlαΔ::LEU2, GPA1::NatMX, ura3Δ::pFUS1-yEVenus*). All the derivative strains are identified by their yGIL prefix and the number in the Lang Lab yeast collection. Mutant strains were constructed using CRISPR-Cas9 as described previously (Fisher et al. 2019). Repair oligonucleotide templates were generated by amplifying 500 bp gBlocks (IDT) that contained the point mutation and a synonymous PAM site substitution. We co-transformed a high-copy plasmid that contains the Cas9 gene and the guide RNA expression cassette (pML104; Addgene #67,638) (Laughery et al. 2015) and the linear repair template into yGIL432 (*MAT**a***) and yGIL646 (*MAT*α) strains. We designed the following sgRNA; *snt1*-A168S (5′-TGG AGCGTTT GATAATGCCG AGG-3′), *snt1*-R1009K (5′-ATGGCTCTAT AAGACCATTT GGG-3′), *sec23*-R592I (5′-TTGGGATCTT CTTAAATAAT AGG-3′), and *ira1*-S700P (5′-GAAGAGATTC TACAACTTGT TGG-3′). After editing, we removed the plasmid on media containing 5-FOA. Diploid mutants were generated by crossing each mutant strain with the opposite mating type mutant strain or wild-type strain to produce homozygotes and heterozygotes, respectively. Crosses were sporulated to confirm diploid strains. All plasmids and strain construction were confirmed by Sanger sequencing (Genscript).

Evolution Experiment

Long-term evolution was performed as described previously (Marad et al. 2018). Briefly, the ancestral diploid strain, yGIL672, was grown to saturation in YPD (yeast extract, peptone, dextrose) medium. A dilution of $1:2^{10}$ was used to seed 48 replicate populations in a single round bottom 96-well plate. The cultures were propagated for 4,000 generations in YPGal medium (yeast extract, peptone, 2% galactose) containing ampicillin (100 mg/mL) and tetracycline (25 mg/mL) to prevent bacterial contamination. The cultures were incubated at 30 °C in an unshaken 96-well plate. Every 24 h, the populations were diluted 1:1,024 by serial dilution 1:32 (4 μl into 125 μl) × 1:32 (4 μl into 125 μl) into a new YPGal 96-well plate. This regime corresponds to 10 generations of growth per day at an effective population size of $\sim 10^5$. The long-term experimental evolution was performed using the Biomek Liquid Handler. Approximately every 50 generations, populations were cryo-archived in 15% glycerol at − 80 °C.

Competitive Fitness Assays

To measure the effect of evolved mutations we used flow-cytometry-based competitive fitness assay as described previously (Buskirk et al. 2017). We used for the competition the reference strains; yGIL519 (*MAT**a***), yGIL699 (*MAT*α), and yGIL702 (*MAT**a***/α). These strains have the ancestral background with constitutive ymCitrine integrated at the *URA3* locus. For all the evolved alleles, we performed the competition in YPD and YPGal under identical conditions. Diploid and haploid strains were competed in independent 96-well plates in an identical fashion to the evolution experiment. The reference and the experimental strains were mixed 1:1 at Generation 0 using a Biomek Liquid handler. The assays were performed for 50 generations and sampled every 10 generations. To measure density using flow-cytometry (BD FACSCanto II), we transferred 4 μL of each sample into 60μL of PBS and stored at 4 °C for 1 day. Data were analyzed in FlowJo 10.3. The selective coefficient was calculated as the slope of the change in the natural log ratio between query and reference strains. For each fitness measurement, we performed between 4–6 independent biological replicates and one technical replicate.

Whole-Genome Sequencing

Each population, from generation 4,000, was struck to singles colonies on YPGal and two clones were isolated for sequencing. Clones were grown to saturation in YPGal and total genomic DNA was isolated for each sample using phenol–chloroform extraction and ethanol precipitation. We used the Nextera sequencing library preparation kit as described previously (Buskirk et al. 2017). Sequencing was performed on an Illumina HiSeq 2500 sequencer with 150-nucleotide paired-end reads by the Sequencing Core Facility within the Lewis-Sigler Institute for Integrative Genomics at Princeton University.

The Oxford Nanopore MinION Genomic DNA Sequencing Kit (SQK-LSK109) was used to prepare the DNA libraries of 8 evolved clones. Briefly, we performed DNA extraction using a QIAGEN 100/G. One microgram of DNA per sample was diluted in 48μL of water. End-repair was performed using NEBNext FFPE Repair Mix and the product was purified using 60 μl of Agencourt AMPure XP beads. End-prepped gDNA was quantified using the Qubit High Sensitivity assay. dA-tailing was performed using NEBNext dA-tailing module. A ligation reaction was then performed by adding 2.5μL of the Native Barcode (EXP-PBC001 and

EXP-PBC096) and 25μL of Blunt/TA Ligase Master Mix. The adapter-ligated DNA was purified using Agencourt AMPure XP beads and washed with long fragment buffer. DNA was quantified using a Qubit and then loaded on to Minion R9.4.1 (product code FLO-MIN106D R9) flow cells.

Sequencing Analysis Pipeline

Raw Illumina sequencing data were concatenated and demultiplexed using barcode_splitter 0.18.6 from L. Parsons (Princeton University). Adapter sequences were trimmed using trimmomatic/0.36 (Bolger et al. 2014) using PE -phred33 parameter. Each sample was aligned to the complete and annotated W303 genome (Matheson et al. 2017) using BWA-MEM, v.0.7.15 (Li and Durbin 2009). Each clone was sequenced to an average depth of approximately 50X coverage (Supplementary Fig. 1). Common variants were called using FreeBayes/1.1.0 (Garrison and Marth 2012), using default parameters. Variants common were filtered using the VCFtools/0.1.15 vcf-isec function (v.0.1.12b). Individual VCF files were annotated using SnpEff/5.0 using -formatEff flag (Cingolani et al. 2012). Manually we did a more punctual filtering of common variants by viewing BAM files using Integrated Genome Viewer (Broad Institute). We removed the variant calls found in low complexity regions (TY elements, centromeres, and telomeric regions) and with less than 5X coverage. Only nuclear mutations were analyzed. We used R package *idiogramFISH* to plot the distribution of our evolved mutations. Zygosity was determined by establishing a cut-off of mutation frequency values above 0.9 and p-values < 0.001. If both parameters were satisfied, we called those mutations homozygous. Copy Number Variants (CNVs) were identified using ControlFREEC version 11.5 (Boeva et al. 2012). All the.txt outputs were merged into one data frame to remove all the common calls. We applied the following criteria to filtered CNVs: the variant is calling more than 10 times, had length less than 5 kb, and variants that were located close to telomeres and centromeres (5 kb of distance) regions. CNVs and aneuploidies were corroborated by visual inspection of chromosome coverage plots created in R. Briefly, we used samtools-depth to calculate per-site depth from the sorted-bam files. We divided the median chromosome coverage by the median genome-wide coverage using non-overlapping 1000 bp window size and 500 nt step size. The total coverage of the genome was normalized to 2 (diploid population). The same analysis was used to estimate copy number of the 2-micron plasmid. Copy number of mitochondrial DNA was estimated using the same sliding window approach but only from the *ATP6*, *COX2*, and *COX3* regions (De Chiara et al. 2020) to avoid overcounting the highly repetitive sequences in the mitochondrial genome. For Nanopore sequencing, we performed basecalling and

demultiplex barcode using guppy/3.1.5. We aligned reads to the S288C reference using the long-read mapper ngmlr/0.2.7 and identified structural variants using Sniffles (Sedlazeck et al. 2018). To visualize chromosome coverage, we used the same methodology described for Illumina data. For glucose-evolved populations, we performed the same analysis as galactose. However, the whole-genome sequencing was performed at Generation 2,000.

Gene Ontology analysis was conducted using Gene Ontology Term Finder (https://www.yeastgenome.org/) and PANTHER (http://pantherdb.org/), both analysis were conducted on Sep, 2022.

Identification of Common Targets

The p-values of coding genes hit by a mutation just by chance were calculated using the Poisson distribution (Fisher et al. 2018). We determined the probability that chance alone explains the observed number of mutations across all 5,800 genes by assuming a random Poisson distribution of CDS mutations weighted by the length of the gene across the 8,453,525 bp genome-wide CDS. First, we determined p-values of the 1,040 CDS mutations without mutation type distinction. However, to increase the statistical power, we also performed the same statistical analysis but focus on nonsynonymous CDS mutation. Final common targets of selection were defined as genes with three or more nonsynonymous CDS mutations and a corresponding probability of less than 0.1%. To determine if the targets of selection are unique to galactose, we compare the p-values with prior glucose evolution experiments (Marad et al. 2018). To determine the targets of selection for each condition, we calculated the ratio between probabilities (Supplementary Data).

Halo Assay

Killer phenotype was performed using the protocol described previously (Buskirk et al. 2020). Assay was performed using YPD agar that had been buffered to pH 4.5 (citrate–phosphate buffer), dyed with methylene blue (0.003%), and poured into a 1-well rectangular cell culture plate. Killing ability was assayed against a hypersensitive tester strain (yGIL1097). The hypersensitive tester was grown to saturation, diluted 1:10, and spread (150 ml) evenly on the buffered agar. Glucose and galactose-evolved populations were grown to saturation, concentrated five-fold, and spotted (2 μL) using liquid handler (Biomek FX). Plates were incubated at room temperature for 3 days before assessment. Killer phenotype was scored according to the scale as shown in Buskirk et al. 2020.

Statistical Analyses

All statistical analyses reported were performed using tools in the R Stats package in R v.4.0.2. All plots were produced in R using the ggplot2 package (Wickham et al. 2016).

Declarations

Conflict of interest The authors declare no competing interests.

References

Acar M, Becskei A, Van Oudenaarden A (2005) Enhancement of cellular memory by reducing stochastic transitions. Nature 435(7039):228–232

Acosta PB, Gross KC (1995) Hidden sources of galactose in the environment. Eur J Pediatr 154(2):S87–S92

Aggeli D, Marad DA, Liu X, Buskirk SW, Levy SF, Lang GI (2022) "Overdominant and partially dominant mutations drive clonal adaptation in diploid Saccharomyces cerevisiae." Genetics 221(2):iyac061

Bailey SF, Hinz A, Kassen R (2014) Adaptive synonymous mutations in an experimentally evolved Pseudomonas fluorescens population. Nat Commun 5(1):1–7

Bakerlee CW, Phillips AM, Ba ANN, Desai MM (2021) Dynamics and variability in the pleiotropic effects of adaptation in laboratory budding yeast populations. Elife 10:e70918

Boeva V, Popova T, Bleakley K, Chiche P, Cappo J, Schleiermacher G, Janoueix-Lerosey I, Delattre O, Barillot E (2012) Control-FREEC: a tool for assessing copy number and allelic content using next-generation sequencing data. Bioinformatics 28(3):423–425

Boles E, Hollenberg CP (1997) The molecular genetics of hexose transport in yeasts. FEMS Microbiol Rev 21(1):85–111

Bolger AM, Lohse M, Usadel B (2014) Trimmomatic: a flexible trimmer for Illumina sequence data. Bioinformatics 30(15):2114–2120

Boocock J, Sadhu MJ, Durvasula A, Bloom JS, Kruglyak L (2021) Ancient balancing selection maintains incompatible versions of the galactose pathway in yeast. Science 371(6527):415–419

Broach JR (2012) Nutritional control of growth and development in yeast. Genetics 192(1):73–105

Buskirk SW, Peace RE, Lang GI (2017) Hitchhiking and epistasis give rise to cohort dynamics in adapting populations. Proc Natl Acad Sci U S A 114(31):8330–8335

Buskirk SW, Rokes AB, Lang GI (2020) Adaptive evolution of nontransitive fitness in yeast. Elife 9:e62238

Chen P, Zhang J (2020) Antagonistic pleiotropy conceals molecular adaptations in changing environments. Nat Ecol Evol 4(3):461–469

Cingolani P, Platts A, Wang LL, Coon M, Nguyen T, Wang L, Land SJ, Lu X, Ruden DM (2012) A program for annotating and predicting the effects of single nucleotide polymorphisms, SnpEff: SNPs in the genome of Drosophila melanogaster strain w1118; iso-2; iso-3. Fly 6(2):80–92

Conrad M, Schothorst J, Kankipati HN, Van Zeebroeck G, Rubio-Texeira M, Thevelein JM (2014) Nutrient sensing and signaling in the yeast Saccharomyces cerevisiae. FEMS Microbiol Rev 38(2):254–299

De Chiara M, Friedrich A, Barré B, Breitenbach M, Schacherer J, Liti G (2020) Discordant evolution of mitochondrial and nuclear yeast genomes at population level. BMC Biol 18(1):1–15

Duan S-F, Han P-J, Wang Q-M, Liu W-Q, Shi J-Y, Li K, Zhang X-L, Bai F-Y (2018) The origin and adaptive evolution of domesticated populations of yeast from Far East Asia. Nat Commun 9(1):1–13

Escalante-Chong R, Savir Y, Carroll SM, Ingraham JB, Wang J, Marx CJ, Springer M (2015) Galactose metabolic genes in yeast respond to a ratio of galactose and glucose. Proc Natl Acad Sci 112(5):1636–1641

Fendt S-M, Sauer U (2010) Transcriptional regulation of respiration in yeast metabolizing differently repressive carbon substrates. BMC Syst Biol 4(1):1–11

Fisher KJ, Buskirk SW, Vignogna RC, Marad DA, Lang GI (2018) Adaptive genome duplication affects patterns of molecular evolution in Saccharomyces cerevisiae. PLoS Genet 14(5):e1007396

Fisher KJ, Kryazhimskiy S, Lang GI (2019) Detecting genetic interactions using parallel evolution in experimental populations. Philos Trans R Soc Lond B Biol Sci 374(1777):20180237

Fu S, Watkins SM, Hotamisligil GS (2012) The role of endoplasmic reticulum in hepatic lipid homeostasis and stress signaling. Cell Metab 15(5):623–634

Galeota-Sprung B, Fernandez A, Sniegowski P (2022) Changes to the mtDNA copy number during yeast culture growth. Royal Soc Open Sci 9(7):211842

Garrison, E. and G. Marth (2012). "Haplotype-based variant detection from short-read sequencing." arXiv preprint arXiv:1207.3907.

Gresham D, Desai MM, Tucker CM, Jenq HT, Pai DA, Ward A, DeSevo CG, Botstein D, Dunham MJ (2008) The repertoire and dynamics of evolutionary adaptations to controlled nutrient-limited environments in yeast. PLoS Genet 4(12):e1000303

Harrison M-C, LaBella AL, Hittinger CT, Rokas A (2021) The evolution of the GALactose utilization pathway in budding yeasts. Trends Genet 38:97–106. https://doi.org/10.1016/j.tig.2021.08.013

Hittinger CT, Carroll SB (2007) Gene duplication and the adaptive evolution of a classic genetic switch. Nature 449(7163):677–681

Hong J, Gresham D (2014) Molecular specificity, convergence and constraint shape adaptive evolution in nutrient-poor environments. PLoS Genet 10(1):e1004041

Hong K-K, Nielsen J (2013) Adaptively evolved yeast mutants on galactose show trade-offs in carbon utilization on glucose. Metab Eng 16:78–86

Hong K-K, Vongsangnak W, Vemuri GN, Nielsen J (2011) Unravelling evolutionary strategies of yeast for improving galactose utilization through integrated systems level analysis. Proc Natl Acad Sci 108(29):12179–12184

Jacob F, Monod J (1961) Genetic regulatory mechanisms in the synthesis of proteins. J Mol Biol 3(3):318–356

Jerison ER, Nguyen Ba AN, Desai MM, Kryazhimskiy S (2020) Chance and necessity in the pleiotropic consequences of adaptation for budding yeast. Nature Ecol Evol 4(4):601–611

Johnson MS, Gopalakrishnan S, Goyal J, Dillingham ME, Bakerlee CW, Humphrey PT, Jagdish T, Jerison ER, Kosheleva K, Lawrence KR, Min J, Moulana A, Phillips AM, Piper JC, Purkanti R, Rego-Costa A, McDonald MJ, Nguyen Ba AN, Desai MM (2021) Phenotypic and molecular evolution across 10,000 generations in laboratory budding yeast populations. Elife. https://doi.org/10.7554/eLife.63910

Kao KC, Sherlock G (2008) Molecular characterization of clonal interference during adaptive evolution in asexual populations of Saccharomyces cerevisiae. Nat Genet 40(12):1499–1504

Kristofich J, Morgenthaler AB, Kinney WR, Ebmeier CC, Snyder DJ, Old WM, Cooper VS, Copley SD (2018) Synonymous mutations make dramatic contributions to fitness when growth is limited by a weak-link enzyme. PLoS Genet 14(8):e1007615

Kvitek DJ, Sherlock G (2013) Whole genome, whole population sequencing reveals that loss of signaling networks is the major adaptive strategy in a constant environment. PLoS Genet 9(11):e1003972

Lang GI, Botstein D (2011) A test of the coordinated expression hypothesis for the origin and maintenance of the GAL cluster in yeast. PLoS ONE 6(9):e25290

Lang GI, Rice DP, Hickman MJ, Sodergren E, Weinstock GM, Botstein D, Desai MM (2013) Pervasive genetic hitchhiking and clonal interference in forty evolving yeast populations. Nature 500(7464):571–574

Laughery MF, Hunter T, Brown A, Hoopes J, Ostbye T, Shumaker T, Wyrick JJ (2015) New vectors for simple and streamlined CRISPR–Cas9 genome editing in Saccharomyces cerevisiae. Yeast 32(12):711–720

Lee KS, Hong ME, Jung SC, Ha SJ, Yu BJ, Koo HM, Park SM, Seo JH, Kweon DH, Park JC (2011) Improved galactose fermentation of Saccharomyces cerevisiae through inverse metabolic engineering. Biotechnol Bioeng 108(3):621–631

Lee KB, Wang J, Palme J, Escalante-Chong R, Hua B, Springer M (2017) Polymorphisms in the yeast galactose sensor underlie a natural continuum of nutrient-decision phenotypes. PLoS Genet 13(5):e1006766

Legras J-L, Galeote V, Bigey F, Camarasa C, Marsit S, Nidelet T, Sanchez I, Couloux A, Guy J, Franco-Duarte R (2018) Adaptation of S. cerevisiae to fermented food environments reveals remarkable genome plasticity and the footprints of domestication. Mol Biol Evol 35(7):1712–1727

Li H, Durbin R (2009) Fast and accurate short read alignment with Burrows-Wheeler transform. Bioinformatics 25(14):1754–1760

Li Y, Venkataram S, Agarwala A, Dunn B, Petrov DA, Sherlock G, Fisher DS (2018) Hidden complexity of yeast adaptation under simple evolutionary conditions. Curr Biol 28(4):515-525.e516

Marad DA, Buskirk SW, Lang GI (2018) Altered access to beneficial mutations slows adaptation and biases fixed mutations in diploids. Nat Ecol Evol 2(5):882–889

Matheson K, Parsons L, Gammie A (2017) "Whole-genome sequence and variant analysis of w303, a widely-used strain of saccharomyces cerevisiae." G3 (bethesda) 7(7):2219–2226

Nair A, Sarma SJ (2021) The impact of carbon and nitrogen catabolite repression in microorganisms. Microbiol Res 251:126831

New AM, Cerulus B, Govers SK, Perez-Samper G, Zhu B, Boogmans S, Xavier JB, Verstrepen KJ (2014) Different levels of catabolite repression optimize growth in stable and variable environments. PLoS Biol 12(1):e1001764

Ostrowski EA, Rozen DE, Lenski RE (2005) Pleiotropic effects of beneficial mutations in Escherichia coli. Evolution 59(11):2343–2352

Peng W, Liu P, Xue Y, Acar M (2015) Evolution of gene network activity by tuning the strength of negative-feedback regulation. Nat Commun 6(1):1–9

Quarterman J, Skerker JM, Feng X, Liu IY, Zhao H, Arkin AP, Jin Y-S (2016) Rapid and efficient galactose fermentation by engineered Saccharomyces cerevisiae. J Biotechnol 229:13–21

Ronen M, Botstein D (2006) Transcriptional response of steady-state yeast cultures to transient perturbations in carbon source. Proc Natl Acad Sci 103(2):389–394

Roop JI, Chang KC, Brem RB (2016) Polygenic evolution of a sugar specialization trade-off in yeast. Nature 530(7590):336–339

Scott AL, Richmond PA, Dowell RD, Selmecki AM (2017) The influence of polyploidy on the evolution of yeast grown in a sub-optimal carbon source. Mol Biol Evol 34(10):2690–2703

Sedlazeck FJ, Rescheneder P, Smolka M, Fang H, Nattestad M, Von Haeseler A, Schatz MC (2018) Accurate detection of complex structural variations using single-molecule sequencing. Nat Methods 15(6):461–468

Sellick CA, Campbell RN, Reece RJ (2008) Galactose metabolism in yeast—structure and regulation of the Leloir pathway enzymes and the genes encoding them. Int Rev Cell Mol Biol 269:111–150

Slepak T, Tang M, Addo F, Lai K (2005) Intracellular galactose-1-phosphate accumulation leads to environmental stress response in yeast model. Mol Genet Metab 86(3):360–371

Sood V, Brickner JH (2017) Genetic and epigenetic strategies potentiate Gal4 activation to enhance fitness in recently diverged yeast species. Curr Biol 27(23):3591-3602.e3593

Sunshine AB, Payen C, Ong GT, Liachko I, Tan KM, Dunham MJ (2015) The fitness consequences of aneuploidy are driven by condition-dependent gene effects. PLoS Biol 13(5):e1002155

Swamy K, Zhou N (2019) Experimental evolution: its principles and applications in developing stress-tolerant yeasts. Appl Microbiol Biotechnol 103(5):2067–2077

Tamanoi F (2011) Ras signaling in yeast. Genes. Cancer 2:210–215

Torres EM, Sokolsky T, Tucker CM, Chan LY, Boselli M, Dunham MJ, Amon A (2007) Effects of aneuploidy on cellular physiology and cell division in haploid yeast. Science 317(5840):916–924

van den Brink J, Akeroyd M, van der Hoeven R, Pronk J, De Winde J, Daran-Lapujade P (2009) Energetic limits to metabolic flexibility: responses of Saccharomyces cerevisiae to glucose–galactose transitions. Microbiology 155(4):1340–1350

Venkataram S, Dunn B, Li Y, Agarwala A, Chang J, Ebel ER, Geiler-Samerotte K, Herissant L, Blundell JR, Levy SF, Fisher DS, Sherlock G, Petrov DA (2016) Development of a comprehensive genotype-to-fitness map of adaptation-driving mutations in yeast. Cell 166(6):1585-1596.e1522

Vignogna RC, Buskirk SW, Lang GI (2021) Exploring a local genetic interaction network using evolutionary replay experiments. Mol Biol Evol 38(8):3144–3152

Voordeckers K, Kominek J, Das A, Espinosa-Cantu A, De Maeyer D, Arslan A, Van Pee M, van der Zande E, Meert W, Yang Y (2015) Adaptation to high ethanol reveals complex evolutionary pathways. PLoS Genet 11(11):e1005635

Wang J, Atolia E, Hua B, Savir Y, Escalante-Chong R, Springer M (2015) Natural variation in preparation for nutrient depletion reveals a cost–benefit tradeoff. PLoS Biol 13(1):e1002041

Wenger JW, Piotrowski J, Nagarajan S, Chiotti K, Sherlock G, Rosenzweig F (2011) Hunger artists: yeast adapted to carbon limitation show trade-offs under carbon sufficiency. PLoS Genet 7(8):e1002202

Wickham H, Chang W, Wickham MH (2016) "Package 'ggplot2'". Create elegant data visualisations using the grammar of graphics. Version 2(1):1–189

Yona AH, Manor YS, Herbst RH, Romano GH, Mitchell A, Kupiec M, Pilpel Y, Dahan O (2012) Chromosomal duplication is a

transient evolutionary solution to stress. Proc Natl Acad Sci 109(51):21010–21015

Zaman S, Im Lippman S, Zhao X, Broach JR (2008) How saccharomyces responds to nutrients. Annu Rev Genet 42:27–81